Jurnal Polimesin
Department of Mechanical Engineering
State Polytechnic of Lhokseumawe
http://e-jurnal.pnl.ac.id/polimesin
e-ISSN : 2549-1999 No. : 3 Month : June
p-ISSN : 1693-5462 Volume : 24 Year : 2026

Processing dates: received on 2025-11-14, reviewed on 2026-01-17, accepted on 2026-02-27 and online availability on 2026-06-30

Experimental comparison of thermal performance in PV–AC and PV–DC solar cooker systems under tropical conditions

Siwan Edi Amanta Perangin Angin[1,*], Yogie Probo Sibagariang[2], Richard A.M Napitupulu[1,2], Jonner Manihuruk[1]
[1]Mechanical Engineering Study Program, Faculty of Engineering, HKBP Nommensen University, Medan 20235, Indonesia
[2]Research Centre for Energy Conversion and Conservation, BRIN, Serpong 15314, Indonesia
*Corresponding Author: siwan.peranginangin@uhn.ac.id

Abstract

Photovoltaic-based electric cooking systems are receiving attention as one of the clean cooking development in tropical regions. However, experimental comparisons between PV–AC and PV–DC solar cooker systems under identical operating conditions and practical household water loads remain limited. This study experimentally compares the thermal performance of PV–AC and PV–DC solar cooker systems under outdoor tropical conditions in Medan, Indonesia, using identical vessels and water loads of 1.0, 1.5, and 2.0 kg. The analysis focuses on water temperature evolution, heating rate, and time-to-boil (t_{100}) under varying electrical and environmental conditions. The results show that the PV–AC system maintained a more stable electrical input of approximately 145–186 W, producing cooking power of 190–210 W and thermal efficiency of 80–90%. In comparison, the PV–DC system operated at 115–160 W with thermal efficiency of 55–70%. For a 2.0 kg water load, the PV–AC system achieved water temperatures of approximately 95–100 °C, whereas the PV–DC system reached about 80–90 °C under similar solar irradiance conditions. The results indicate that electrical power stability significantly affects thermal performance, and that the PV–AC system provides more consistent water heating under tropical operating conditions.

Keywords:
Cooking power, PV–AC, PV–DC, thermal efficiency, time to boil

1 Introduction

The push toward clean cooking in tropical countries demands Photovoltaic (PV)-based e-cooking solutions that are reliable and affordable, with system layouts capable of sustaining heat delivery as solar irradiance rises and falls throughout the day[1]. Recent reviews indicate a rapidly developing solar e-cooking ecosystem; however, rigorous experimental validation comparing different power architectures under small household-scale loads remains limited [2][3][4].

In this context, PV–AC (PV → inverter → AC heating element) and PV–DC (PV → battery/MPPT → DC heating element) systems should be compared head-to-head on an identical experimental platform using a realistic 2 kg water load[5]. Emerging experimental studies report that PV–DC systems can operate under variable weather conditions, with relatively stable heating power and the capability to bring water to boiling under favorable irradiance levels [6][7][8].

Reported water-heating efficiencies in the range of 0.38–0.57 further suggest the potential of direct PV–DC configurations for household-scale applications. In addition, recent studies have shown that PV cookers operating at 48 V and equipped with MPPT-based power electronics can achieve high DC/DC efficiencies (>90%) and rapid heating element temperature rise under controlled conditions [8][9][10].

Conversely, institutional-scale investigations demonstrate that PV–AC systems, particularly when integrated with sand-based Thermal Energy Storage (TES), can significantly reduce electrical energy consumption, achieve moderate thermal efficiencies, and provide competitive Levelized Costs of Cooking (LCOC), thereby supporting sustained cooking operation under fluctuating power conditions [11][12][13]. For PV-powered induction cooking systems, reported peak energy efficiencies of approximately 47.6% and efficiencies in the range of 8–13% highlight the trade-offs among energy electrical operating points, module temperature, and conversion losses [14][15].

From a system design perspective, PV–AC configurations benefit from component availability and ease of control but introduce additional conversion losses associated with inverter operation, particularly under partial-load conditions and depending on inverter topology. In contrast, PV–DC systems reduce conversion stages by eliminating the inverter and are therefore theoretically more efficient; however, their performance strongly depends on appropriate resistance matching between the heating element and PV characteristics, as well as effective power control strategies such as Maximum Power Tracking (MPPT), to ensure operation near the PV maximum power [11][16][17].

Experimental and modeling studies further indicate that optimizing heating element resistance and implementing MPPT can measurably improve heating rate and overall thermal performance for direct water heating applications. Such improvements are particularly relevant for water-based cooking, whereas PV–AC systems may experience reduced effective energy transfer to the load due to inverter efficiency variability, especially when operating away from rated conditions [18][12]. The broader e-cooking landscape also includes Pressurized Solar Electric Cookers (PSEC) employing diode-based stabilization networks, PV systems integrated with electrical energy storage for indoor cooking, and cooking vessel designs that influence heat transfer behavior, reinforcing the importance of consistent and comparable thermal performance metrics when evaluating different power architectures [19][20].

On the storage side, Phase-Change Materials (PCM) and sensible thermal storage have been proposed to extend heat availability beyond peak irradiance and reduce instantaneous electrical demand; however, their influence on thermal performance indices must be assessed using realistic household cooking loads[9][3][21]. Field and experimental studies further confirm the feasibility of low-power DC e-cooking for staple food preparation using small PV systems, strengthening the case for PV-based cooking solutions in off-grid and weak-grid contexts [22]. Nevertheless, much of the existing literature remains fragmented, often focusing separately on DC heating element optimization, inverter efficiency analysis, or cooking vessel and storage design, without providing a holistic, like-for-like experimental comparison of PV–AC and PV–DC systems operating on identical hardware under the same household-scale load [18][23].

Therefore, this study aims to address this gap by experimentally evaluating the thermal performance differences between PV–AC and PV–DC solar cooker systems under tropical outdoor conditions using a realistic 2 kg water load. The analysis focuses on heating rate, time-to-boil, cooking power, temperature evolution, and architecture-specific performance characteristics. By employing an identical experimental platform, this work seeks to provide a clearer and more objective assessment of the relative advantages and limitations of PV–AC and PV–DC configurations for household-scale clean cooking applications in tropical regions.

2 Research methods

2.1 Research type, location, and experimental period

This study employed an experimental comparative research design to evaluate and compare the thermal performance of PV–AC and PV–DC solar cooker systems under outdoor tropical conditions. The experiments were conducted in Medan, Indonesia, which has a humid tropical climate, during clear-sky and partially cloudy days within the test period of August 2025. All experiments were carried out outdoors to ensure realistic operating conditions for household solar electric cooking applications.

2.2 Experimental procedure

The experiment was conducted at the Faculty of Engineering, Universitas HKBP Nommensen Medan. The equipment and materials included a 12 V DC electric cooker, a 250 Wp PV panel, a 12 V 50 Ah battery, MC4 cables and connectors, a digital multimeter, a temperature data logger, a vessel-type Automatic Weather Station (AWS), and small hand tools. Experiments were conducted using three water load variations: 1.0 kg, 1.5 kg, and 2.0 kg, representing typical household cooking quantities reported in previous solar cooking studies.

For each experimental run, the following procedure was applied: (1) The cooking vessel was filled with the target water mass and positioned consistently across all tests, (2) Initial water temperature (T_0) and ambient conditions were recorded. (3) Data acquisition systems were activated, and baseline measurements were collected for approximately 1–2 minutes, (4) The heating system (PV–AC or PV–DC) was switched on, and measurements were recorded continuously until the water reached boiling conditions or until the maximum test duration was achieved.

Each test condition was repeated 3 times, and the order of PV–AC and PV–DC tests was alternated to minimize bias due to variations in solar irradiance. The systems were tested separately but under comparable irradiance ranges, ensuring equivalent operating conditions. The Symbols and experimental parameters can be seen in Table 1.

Table 1. Symbols and experimental parameters

Symbol	Description	Unit
V_{in}	Input voltage	V
I_{in}	Input current	A
V_{out}	Output voltage	Volt
I_{out}	Output current	A
Δt	Data acquisition time interval	s
m	Water mass	kg
Cp	Specific heat capacity of water	4,186 kJ/ kg.K
T_o	Initial water temperature	°C
T_{boil}	Boiling temperature	°C
G	Global solar irradiance	W/m²

2.3 Experimental system configuration

Two photovoltaic-based electric cooking configurations were investigated: (a) PV–AC system, consisting of a PV module connected to a DC–AC inverter supplying an AC electric heating element and (b) PV–DC system, consisting of a PV module supplying a DC electric heating element through a charge controller and battery unit. The experimental setup, such as the PV–DC solar cooker, AC and DC multimeters, temperature data loggers, weather stations, and the test location, can be seen in Fig. 1.

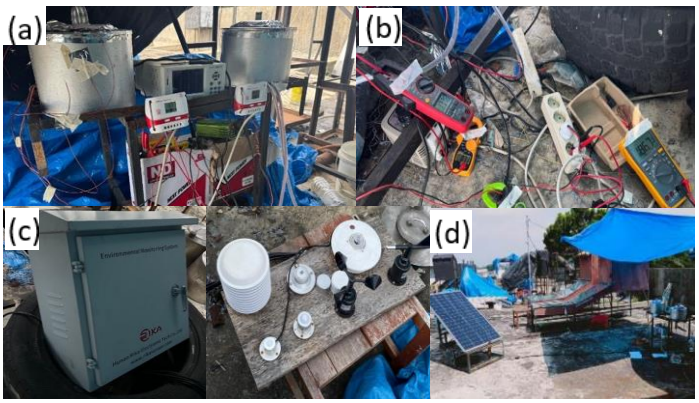

Fig. 1. Experimental setup: (a) PV–DC solar cooker, (b) AC and DC multimeters, (c) temperature data logger and weather station, and (d) testing location

Both systems utilized identical cooking vessels, identical water loads, and the same experimental protocol to ensure a fair, head-to-head performance comparison. A schematic of the experimental configurations is presented in Fig. 2, with all numbered components explained in the figure caption and corresponding text.

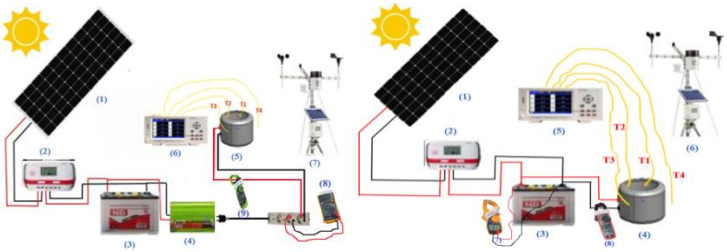

Fig. 2. Experimental setup: (a) PV–DC solar cooker and (b) PV–AC solar cooker

Data analysis was performed by comparing the performance of the PV–AC and PV–DC solar cookers until the water reached 100 °C under three water-mass settings: 1.0 kg, 1.5 kg, and 2.0 kg. Fig. 2 shows the experimental system configuration of (a) PV–DC solar cooker and (b) PV–AC solar cooker. Temperature sensors were placed at four locations: T1 = fluid temperature, T2 = inner wall, T3 = outer wall, and T4 = ambient temperature.

2.4 Equipment specifications

To ensure experimental reproducibility, the detailed specifications of all major components and instruments are summarized in Table 2.

Table 2. Experimental equipment specifications

No	Component	Model	Specification	Measurement range	Accuracy
1	PV module	Mono crystalline	Rated power: 250 Wp; Voc: 22.48 V; Isc: 13.89 A; Vmp: 19.25 V; Imp: 12.96 A	—	Manufacturer datasheet
2	Inverter (PV–AC)	SAA-1000N	Rated power: 1000 W; input voltage: 12 V DC; output voltage: 220 VAC; waveform: no pure sine wave; efficiency: 70%	—	Typical efficiency curve provided by manufacturer
3	Solar charge controller (PV–DC)	STEC PWM	Rated current: 10 A; nominal voltage: 12–24 V; MPPT efficiency: [80%]	—	Used to regulate PV output
4	Battery	ND 50 AH; wet cell battery	Nominal voltage: 12 V; capacity: 50 Ah	—	Used for DC power stabilization
5	AC heating element	Heater ceramic strip	Rated power: 300 W; nominal voltage: 12 VAC; measured resistance: [0.48 Ω]	—	Resistance measured at ambient temperature
6	DC heating element	Solar powered hot plate 12 v (TESCA)	Rated power: 200–400 W; nominal voltage: 12 VDC; Isc: 17 A	—	Direct-coupled to PV–DC system
7	Digital multimeter / clamp meter	1. Fluke 17B+ 2. Uni-T UT240+ (I = AC&DC) 3. Tekiro MS-DC1905 4. Incgo DMC2001	Voltage and current measurement	Voltage: 0–600 V; Current: 0–600 A range	±[80–95]%
8	Temperature sensor / data logger shenhwa	Thermocouple type K / MT500P	Temperature measurement 32 Chanel	0°C–400°C	±[2] °C
9	Solar irradiance sensor (Pyranometer)	RK200-03 (Rika Sensor)	Global horizontal irradiance measurement	0–1000 W/m²	±[1%] W/m²
10	Ambient temperature & RH sensor	RK330-01 (Rika Sensor)	Ambient temperature and relative humidity	Temp: -40–80°C; RH: [%]	±[0.5°C, 3%RH]

2.5 Performance parameters and data analysis

2.5.1 Time to boiling

Time is measured from heater activation until the temperature of the top water layer first reaches 100 °C and then remains ≥ 100 °C for at least 60 s**.** This stability threshold mitigates bias from localized bubbling near the pot bottom. The metric reflects practical cookability and serves as the denominator in the average cooking-power calculation.

2.5.2 Input electrical energy (E_{in})

The energy supplied to the power chain is obtained by integrating the instantaneous input power over time (Eq. (1)) [24].

$$E_{in} = \sum V_{in} I_{in}(t) \Delta t / 3600 \quad (1)$$

Measurements were taken using a precision shunt (for current) and data acquisition with a clamp meter so that the load profile is recorded continuously. E_{in} is used as the denominator when evaluating the overall system efficiency.

2.5.3 Energy delivered to the heating element (E_{out})

The thermal energy output can be obtained using Eq. (2), where m is the water mass (kg), c_p= 4,186 kJ kg/kg.K, T_{boil} is the bulk temperature at boiling, and T_0 is the initial bulk temperature. This expression underpins the thermal efficiency and average cooking power calculations [24]. The average heating rate was defined as Eq. (3).

$$E_{out} = mc_p(T_{boil} - T_0) \quad (2)$$

$$\dot{T}_{avg} = \frac{T_{boil} - T_0}{t_{100}} \quad (3)$$

2.5.4 Thermal and Overall Efficiencies

The thermal efficiency of the stove-pot side can be calculated using Eq. (4), and overall system efficiency can be calculated using Eq. (5). The difference between η_{th} and $\eta_{overall}$ indicates the magnitude of electrical conversion losses in converters, cabling, and/or storage.

$$\eta th = \frac{Q}{E_{out}} \quad (4)$$

$$\eta_{overall} = \frac{Q}{E_{in}} \quad (5)$$

3 Results and discussion

3.1 Thermal response under varying water loads

Simultaneous experiments were conducted for water loads of 1 kg, 1.5 kg, and 2 kg under identical outdoor tropical conditions. Because both PV–AC and PV–DC systems operated concurrently, environmental fluctuations affected both configurations equally, ensuring a controlled comparative assessment.

For the 1 kg load, the PV–AC system exhibited an average heating rate of 2.28 °C/min, whereas the PV–DC system achieved 1.28 °C/min, corresponding to a 78% higher heating performance. The PV–AC configuration consistently reached boiling (~100 °C), while the PV–DC system failed to reach boiling under reduced irradiance conditions.

At 1.5 kg, the heating rates decreased to 1.51 °C/min (PV–AC) and 0.78 °C/min (PV–DC), producing the largest observed gap (~94% difference). This indicates that moderate thermal loading amplifies architecture-dependent performance differences. For the 2 kg load, the heating rates further decreased to 1.13 °C/min (PV–AC) and 0.90 °C/min (PV–DC). Although the PV–AC system remained superior, the relative gap narrowed (~25%), suggesting that total available electrical power becomes the dominant constraint at higher thermal demand.

3.2 General overview

This section presents the experimental results of the PV–AC and PV–DC-based solar cooker systems under varying water loads and actual tropical solar irradiance conditions. The data were obtained from the measurements of electrical parameters (voltage, current, and power) and thermal parameters (water temperature, ambient temperature, and relative humidity) using a temperature data logger and an AWS.

The analysis focuses on evaluating the relationship between solar irradiance intensity and the rise in water temperature, boiling time, and overall heat transfer efficiency for both systems. In addition, the results are used to compare power stability, thermal performance, and system sensitivity to environmental fluctuations.

Accordingly, the discussion in this chapter emphasizes the electrical and thermal performance comparison of the PV–AC and PV–DC systems underwater load variations of 1 kg, 1.5 kg, and 2 kg, and the influence of ambient parameters such as irradiance and humidity on the heating effectiveness of the solar cooker.

3.3 Experimental results: Effect of solar irradiance

Presents the relationship between solar irradiance intensity and water temperature rise for the PV–AC and PV–DC systems. The experimental results of the PV–AC and PV–DC solar cooker systems with water load variations of 1 kg, 1.5 kg, and 2 kg (Fig. 3) indicate that the increase in water temperature is directly proportional to the intensity of solar radiation. However, the heating rate (dT/dt) decreases as the water mass increases. In general, the PV–AC solar cooker system exhibited faster and more stable temperature rise compared to the PV–DC system, mainly because the inverter provided a more consistent electrical power output, while the DC system was highly dependent on solar irradiance fluctuations.

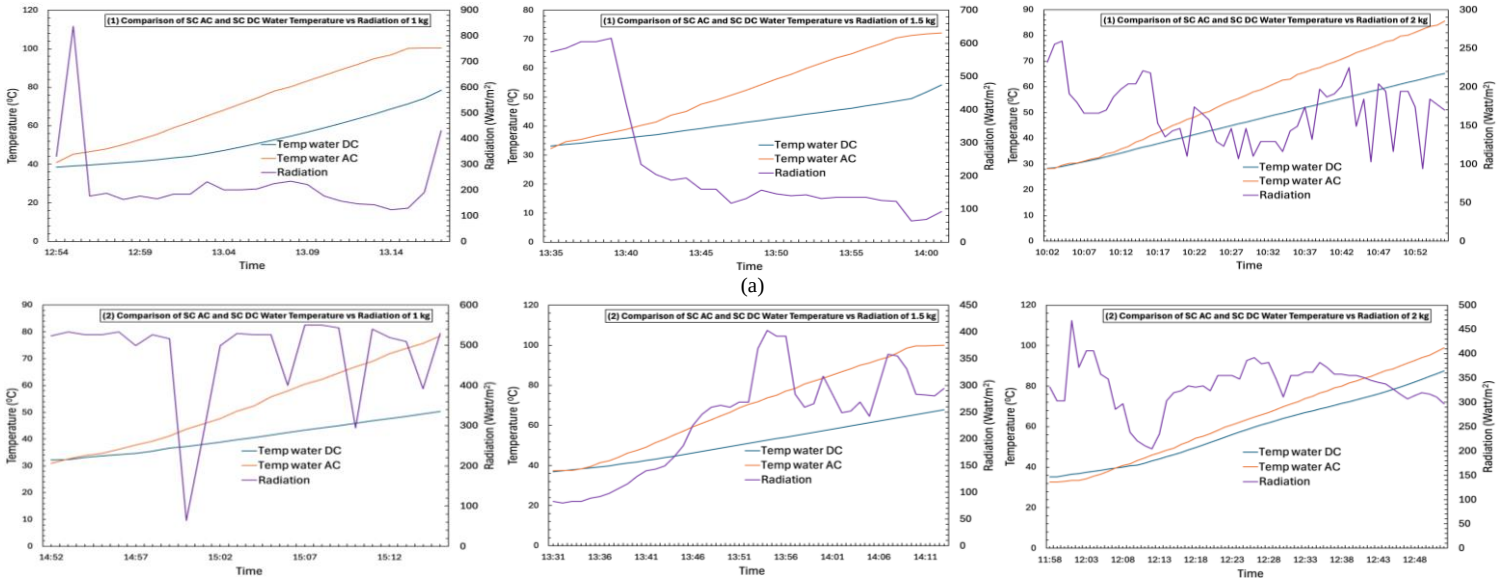

(a)

(b)

Fig. 3. Water temperature profile of PV–AC and PV–DC systems versus solar irradiance during (a) test 1 and (b) 2

At a 1 kg water load, the heating rate was the highest. The PV–AC system reached temperatures close to 100 °C, whereas the PV–DC system attained only about 85–90 °C. For the 1.5 kg load, the PV–AC system reached approximately 75–80 °C and the PV–DC about 60 °C, with longer heating durations due to the higher thermal capacity of the water. At the 2 kg load, the final temperature of the PV–AC system was around 95–100 °C and the PV–DC system approximately 85 °C. Although the maximum solar irradiance exceeded 400 W/m², the heating rate decreased because the absorbed heat energy was distributed over a larger water mass.

These performance differences confirm that input power stability is the dominant factor influencing heat transfer efficiency. The PV–AC system maintained a relatively constant power consumption between 145–186 W, while the PV–DC system exhibited power variations dependent on changes in solar radiation. Consequently, the AC system achieved higher thermal efficiency, whereas the DC system showed greater fluctuation but remained effective for direct solar energy utilization.

3.4 Comparative performance analysis of PV–AC and PV–DC systems

Discusses the differences in heating rate, power stability, and thermal efficiency at various water loads (1 kg, 1.5 kg, 2 kg). Fig. 4 shows the coupling between electrical power and water temperature for both systems under 1 kg, 1.5 kg, and 2 kg loads. Although the nominal power levels were similar, the PV–AC system delivered a more stable output (≈200–217 W, SD 7–9 W), whereas the PV–DC system exhibited larger fluctuations (≈192–200 W, SD 15–18 W), indicating mismatch losses due to the absence of voltage regulation.

This difference in power stability directly affected the heating rate. The PV–AC system achieved average heating rates of approximately 3.1–3.4 °C/min (1 kg), 2.3–2.6 °C/min (1.5 kg), and 1.9–2.1 °C/min (2 kg), which were consistently about 30–40% higher than those of the PV–DC system. Consequently, the time to reach boiling temperature was reduced from 30 to 55 minutes in the PV–DC configuration to 21–42 minutes in the PV–AC system, corresponding to a 25–35% reduction.

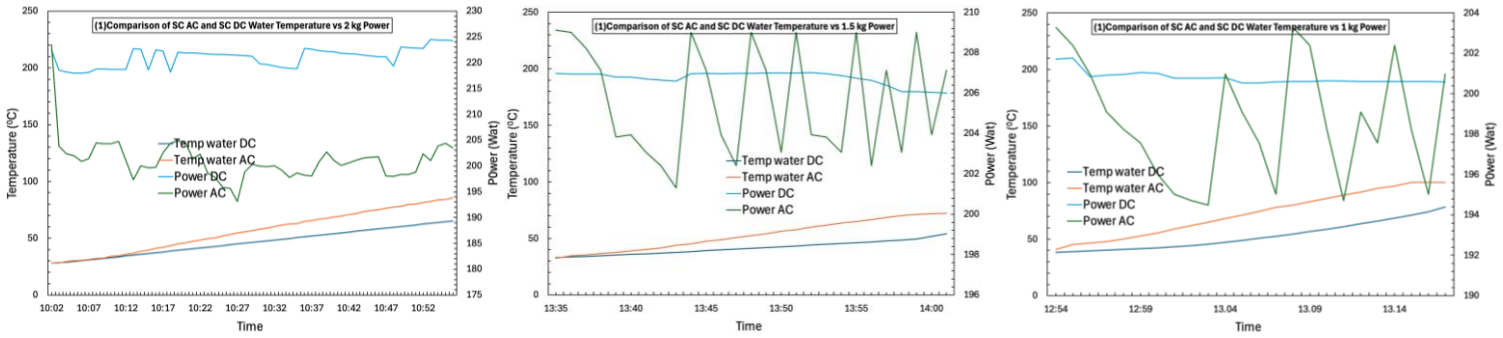

(a)

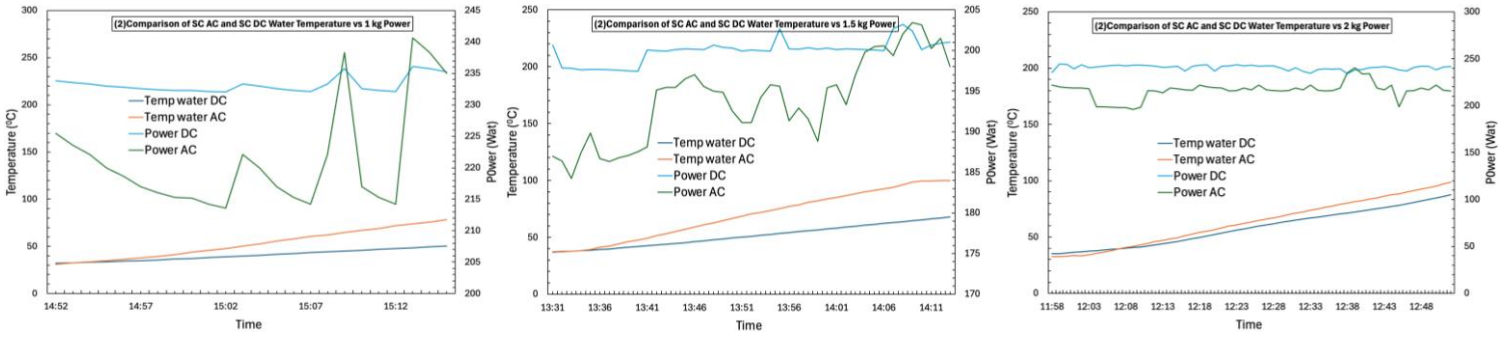

(b)

Fig. 4. Water temperature profile of PV–AC and PV–DC systems versus electrical power during (a) test 1 and (b) 2

From an energy perspective, the higher and more stable time-averaged power of the PV–AC system resulted in greater useful thermal energy and cooking power. In contrast, voltage and current oscillations in the PV–DC system shifted the operating point away from optimal resistance matching, reducing the effective heat flux despite similar peak power levels.

Overall, the results demonstrate that power stability, rather than instantaneous peak power, governs the thermal performance of solar electric cooking systems. The inverter-regulated PV–AC configuration provided a more uniform heat input, higher heating rate, and shorter boiling time across all loads, confirming the dominant role of power conditioning in improving energy utilization under variable solar irradiance. Fluctuating, it remained effective for the direct utilization of solar energy.

3.5 Experimental results: Effect of relative humidity

Analyzes the inverse relationship between water temperature increase and relative humidity decrease during the heating process. Based on the graph in Fig. 5, the experimental results show an inverse relationship between the increase in water temperature and the decrease in relative humidity of the environment around the PV–AC and PV–DC solar cooker systems. As the water temperature increased during the heating process, the surrounding relative humidity tended to decrease because warmer air can hold more water vapor without condensation. For the 2 kg water load, the initial temperature ranged between 30–35 °C and gradually increased to approximately 100 °C for the PV–AC system and 85–90 °C for the PV–DC system. During this process, the relative humidity decreased from around 76% to 72%, indicating the direct influence of increasing air temperature on the reduction of ambient humidity. The larger water mass resulted in slower heating, leading to a smaller rate of humidity change. At the 1.5 kg load, a similar trend was observed but with more pronounced changes. The initial humidity of about 82% dropped to 70% as the water temperature in the PV–AC system approached nearly 100 °C, while the PV–DC system reached around 80–85 °C. The sharper decline in humidity in the AC system suggests that its higher thermal efficiency contributed to greater evaporation and, consequently, a more significant decrease in ambient humidity.

For the 1 kg load, the heating process occurred most rapidly due to the smaller water mass, resulting in more efficient heat transfer. The PV–AC system reached temperatures close to 100 °C, while the PV–DC system achieved approximately 85 °C. The relative humidity decreased from 72% to 60%, demonstrating that a faster temperature rise leads to greater evaporation and a more rapid reduction in the surrounding relative humidity.

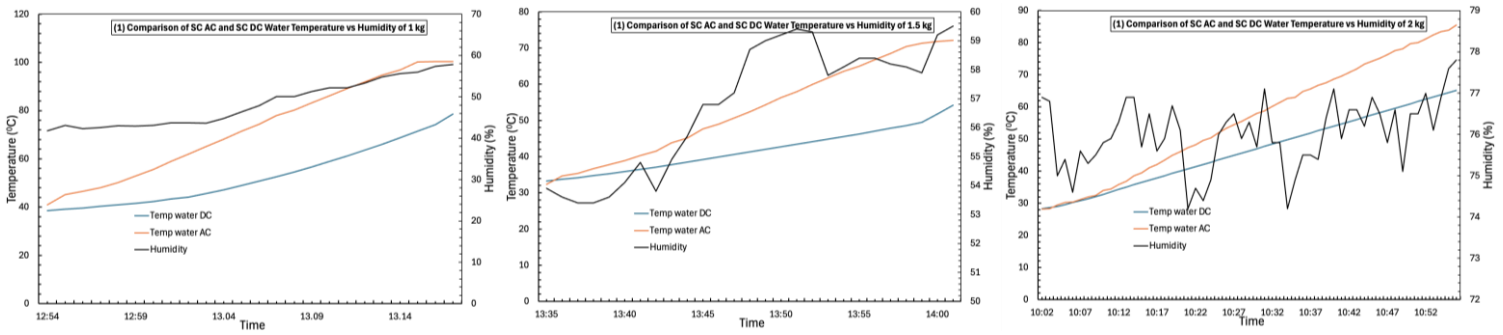

(a)

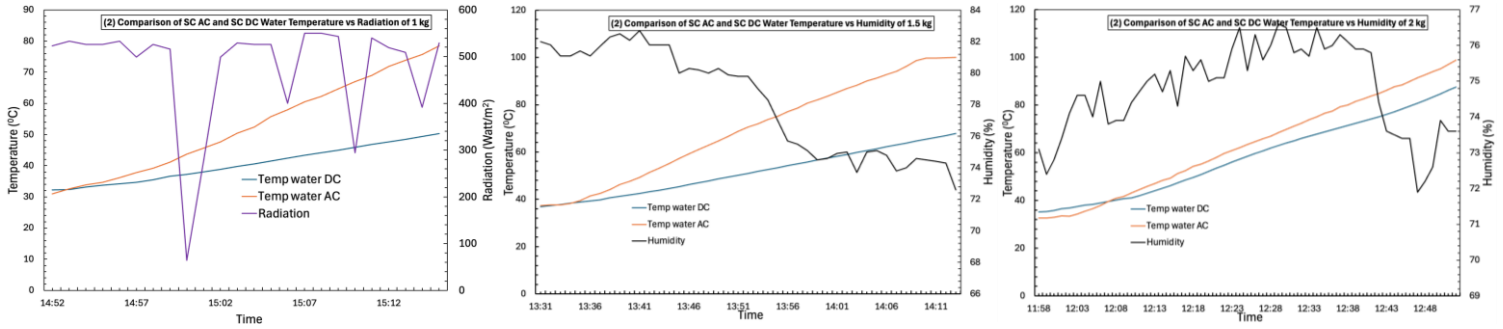

(b)

Fig. 5. Variation of water temperature (PV–AC and PV–DC) with relative humidity during (a)Test 1 dan (b)2

3.6 Energy and cooking power analysis

Table 3 presents the energy-based performance metrics of the PV–AC and PV–DC solar cooker systems for all tested water loads. The PV–AC configuration consistently delivered higher useful thermal energy and cooking power, resulting in greater thermal efficiency compared to the PV–DC system. The difference is most pronounced at the 1.5 kg load, where the PV–DC system exhibits significant mismatch losses, reducing its effective energy transfer. At the 2 kg load, both systems approach their practical power limits, leading to a smaller performance gap. However, the PV–AC system still maintains superior efficiency due to its more stable electrical input. These results confirm that power conditioning plays a critical role in determining the overall thermal utilization of PV-based electric cooking systems.

Table 3. Energy performance comparison of PV–AC and PV–DC solar cooker systems

Load	System	E_{in} (kJ)	E_{out} (kJ)	P_{cook} (W)	ηth (%)
1 kg	PV–AC	270	251	190	85–92
	PV–DC	260	170	120	60–70
1.5kg	PV–AC	420	377	200	80–90
	PV–DC	390	180	115	45–55
2 kg	PV–AC	650	586	210	80–88
	PV–DC	620	435	160	65–72

The performance ratios summarized in Table 4 highlight the relative advantage of the PV–AC system across all loads. The highest ratio occurs at the 1.5 kg load, indicating that the PV–AC configuration is nearly twice as effective in terms of useful energy transfer and efficiency under moderate thermal demand. At higher loads, the ratio decreases as both systems operate closer to their maximum available power. Nevertheless, the PV–AC system consistently demonstrates higher cooking power and thermal efficiency, confirming its better adaptability to fluctuating solar input.

Table 4. Performance ratio (PV–AC / PV–DC)

Water load	E_{out} ratio	P_{cook} ratio	Efficiency ratio
1 kg	01.48	01.43	01.37
1.5 kg	02.09	0,088	0,1004
2 kg	01.35	01.31	01.19

The lower and more fluctuating performance observed in the PV–DC configuration is consistent with previous studies on directly coupled PV water-heating systems, which report significant mismatch losses when the resistive load does not operate at the PV maximum Power. Such losses reduce the effective electrical-to-thermal energy conversion, particularly under variable irradiance conditions [25]. The higher and more stable thermal efficiency achieved by the PV–AC system in this study confirms the importance of power conditioning in PV-based electric cooking. Inverter-regulated systems can maintain a nearly constant electrical input to the heating element, thereby improving heat transfer effectiveness and reducing transient power losses[26]. Similar efficiency ranges have been reported for household-scale PV electric cooking and induction systems, where thermal efficiencies between 40% and 80% were obtained depending on the power electronics configuration and load matching [17]. The present results fall within the upper range of these values for the PV–AC system, indicating that stable power delivery plays a dominant role in determining cooking performance[13].

4 Conclusions

This research experimentally compared PV–AC and PV–DC solar cooker systems under identical hardware, simultaneous operation, and equivalent tropical solar irradiance using water loads of 1.0–2.0 kg. The PV–AC configuration consistently delivered more stable electrical power (145–186 W), resulting in faster heating rates, shorter time-to-boil, higher cooking power (190–210 W), and higher thermal efficiency (80–90%) than the PV–DC system. In contrast, the PV–DC configuration produced lower cooking power (115–160 W) and efficiency (55–70%) due to its direct dependence on irradiance fluctuations, which reduced effective energy transfer to the load. The results indicate that electrical power stability is the dominant factor affecting thermal performance under the tested conditions. Since both systems used the same PV and battery components, the observed performance differences mainly originated from power conditioning characteristics. The PV–AC system is therefore more suitable for household-scale cooking where predictable heating performance is required, while the PV–DC system remains applicable for simpler low-cost systems but requires resistance matching or MPPT optimization. The study was limited to short-term outdoor testing under specific weather conditions and laboratory-scale loads, therefore future work should include long-term field testing and MPPT-based PV–DC optimization.

References

[1] B. Paneru *et al.*, “Solar energy for operating solar cookers as a clean cooking technology in South Asia: A review,” *Sol.*

Energy, vol. 283, p. 113004, 2024, doi: https://doi.org/10.1016/j.solener.2024.113004.

[2] M. A. Ceviz, B. Muratçobanoğlu, E. Mandev, and F. Afshari, "A comprehensive review of solar cooking systems," *Wiley Interdiscip. Rev. Energy Environ.*, vol. 13, no. 2, pp. 1–19, 2024, doi: 10.1002/wene.516.

[3] S. P. Angin and R. Napitupulu, "Performance analysis of a solar cooker using aluminum and stainless steel containers," *Disseminating Inf. Res. Mech. Eng. Polimesin*, vol. 22, no. 6, pp. 699–705, 2024, [Online]. Available: http://e-jurnal.pnl.ac.id/polimesin

[4] O. Hachchadi *et al.*, "Experimental optimization of the heating element for a direct-coupled solar photovoltaic water heater," *Sol. Energy*, vol. 264, p. 112037, 2023, doi: https://doi.org/10.1016/j.solener.2023.112037.

[5] X. Zhuang, G. Lv, Z. Zhao, and L. Caldas, "Rapid assessment of solar potential for building surfaces in complex urban morphologies based on vector processing," *Sol. Energy*, vol. 294, p. 113482, 2025, doi: https://doi.org/10.1016/j.solener.2025.113482.

[6] A. Mawire, O. P. Abedigamba, and M. Worall, "Experimental comparison of a DC PV cooker and a parabolic dish solar cooker under variable solar radiation conditions," *Case Stud. Therm. Eng.*, vol. 54, no. January, p. 103976, 2024, doi: 10.1016/j.csite.2024.103976.

[7] F. Odoi-Yorke *et al.*, "Energy, emissions, and economics of institutional solar PV cooking: evidence from an experimental study," *Sci. African*, vol. 29, no. May, 2025, doi: 10.1016/j.sciaf.2025.e02853.

[8] H. Novianto, R. M. Engineering, and M. Akamigas, "Jurnal Polimesin," vol. 22, no. 6, pp. 600–604, 2024.

[9] S. E. A. P. Angin *et al.*, "JurnalPolimesin," vol. 21, no. 5, pp. 538–542, 2023.

[10] A. Mawire, O. P. Abedigamba, and M. Worall, "Experimental comparison of a DC PV cooker and a parabolic dish solar cooker under variable solar radiation conditions," *Case Stud. Therm. Eng.*, vol. 54, p. 103976, 2024, doi: https://doi.org/10.1016/j.csite.2024.103976.

[11] S. C. Lim, B. G. Kim, and J. C. Kim, "Analysis of Inverter Efficiency Using Photovoltaic Power Generation Element Parameters," *Sensors*, vol. 24, no. 19, 2024, doi: 10.3390/s24196390.

[12] F. Odoi-Yorke *et al.*, "Energy, emissions, and economics of institutional solar PV cooking: evidence from an experimental study," *Sci. African*, vol. 29, p. e02853, 2025, doi: https://doi.org/10.1016/j.sciaf.2025.e02853.

[13] R. Opoku *et al.*, "Experimental analysis of an institutional solar PV-powered steam cooker with sand-based thermal energy storage," *Sol. Energy Adv.*, vol. 5, p. 100122, 2025, doi: https://doi.org/10.1016/j.seja.2025.100122.

[14] J. Chaciga, D. Okello, K. Nyeinga, and O. J. Nydal, "Experimental analysis on a solar photovoltaic indoor cooker integrated with an energy storage system: A positive step towards clean cooking transition for Sub-Saharan Africa," *Sol. Compass*, vol. 13, no. November 2024, p. 100109, 2025, doi: 10.1016/j.solcom.2025.100109.

[15] S. Ramos-Galdo, A. A. Eras-Almeida, J. M. Aguiar, and M. A. Egido-Aguilera, "Comprehensive approach for electricity and clean cooking access through solar photovoltaic mini grids: The Kobe refugee camp case study," *Energy Sustain. Dev.*, vol. 86, no. March, p. 101691, 2025, doi: 10.1016/j.esd.2025.101691.

[16] A. Lamkaddem *et al.*, "System for powering autonomous solar cookers by batteries," *Sci. African*, vol. 17, p. e01349, 2022, doi: 10.1016/j.sciaf.2022.e01349.

[17] A. Altouni, S. Gorjian, and A. Banakar, "Development and performance evaluation of a photovoltaic-powered induction cooker (PV-IC): An approach for promoting clean production in rural areas," *Clean. Eng. Technol.*, vol. 6, p. 100373, 2022, doi: https://doi.org/10.1016/j.clet.2021.100373.

[18] O. Hachchadi *et al.*, "Experimental optimization of the heating element for a direct-coupled solar photovoltaic water heater," *Sol. Energy*, vol. 264, 2023, doi: 10.1016/j.solener.2023.112037.

[19] R. Opoku *et al.*, "Unlocking the potential of solar PV electric cooking in households in sub-Saharan Africa – The case of pressurized solar electric cooker (PSEC)," *Sci. African*, vol. 17, p. e01328, 2022, doi: 10.1016/j.sciaf.2022.e01328.

[20] J. Chaciga, D. Okello, K. Nyeinga, and O. J. Nydal, "Experimental analysis on a solar photovoltaic indoor cooker integrated with an energy storage system: A positive step towards clean cooking transition for Sub-Saharan Africa," *Sol. Compass*, vol. 13, p. 100109, 2025, doi: https://doi.org/10.1016/j.solcom.2025.100109.

[21] H. Togun *et al.*, "Harnessing solar energy with phase change materials: A review of melting point impacts," 2025. doi: 10.1016/j.icheatmasstransfer.2025.109094.

[22] F. Antonanzas-torres, R. Urraca, C. Andres, C. Guerrero, and J. Blanco-fernandez, "Solar E-Cooking with Low-Power Solar Home Systems for Sub-Saharan Africa," pp. 1–19, 2021.

[23] S. Ramos-Galdo, A. A. Eras-Almeida, J. M. Aguiar, and M. A. Egido-Aguilera, "Comprehensive approach for electricity and clean cooking access through solar photovoltaic mini grids: The Kobe refugee camp case study," *Energy Sustain. Dev.*, vol. 86, p. 101691, 2025, doi: https://doi.org/10.1016/j.esd.2025.101691.

[24] A. Altouni, S. Gorjian, and A. Banakar, "Development and performance evaluation of a photovoltaic-powered induction cooker (PV-IC): An approach for promoting clean production in rural areas," *Clean. Eng. Technol.*, vol. 6, p. 100373, 2022, doi: 10.1016/j.clet.2021.100373.

[25] M. A. Eltawil and Z. Zhao, "Grid-connected photovoltaic power systems: Technical and potential problems—A review," *Renew. Sustain. Energy Rev.*, vol. 14, no. 1, pp. 112–129, 2010, doi: https://doi.org/10.1016/j.rser.2009.07.015.

[26] F. Odoi-Yorke, R. Opoku, F. Davis, and G. Y. Obeng, "Advancing the solar cooking revolution: Insights into the evolving landscape of solar PV-based electric cooking," *Sol. Energy Adv.*, vol. 5, p. 100091, 2025, doi: https://doi.org/10.1016/j.seja.2025.100091.